Normal Values of Right Ventricular Size and Function by Real-time 3-Dimensional Echocardiography: Comparison with Cardiac Magnetic Resonance Imaging

Aasha S. Gopal, MD, FACC, Ebere O. Chukwu, MD, Chizor J. Iwuchukwu, MD, Alan S. Katz, MD, Rena S. Toole, RDCS, William Schapiro, RT, and Nathaniel Reichek, MD, *Roslyn and Stony Brook, New York*

Background: **Assessment of right ventricular function by 2-dimensional echocardiography (2DECHO) is difficult because of its complex shape. Real-time 3-dimensional echocardiography (RT3DECHO) may be superior.**

Methods: **End-diastolic volume, end-systolic volume, stroke volume, and ejection fraction obtained by 2DECHO, RT3DECHO short-axis disk summation (DS), and RT3DECHO apical rotation were compared with cardiac magnetic resonance imaging in 71 healthy individuals.**

Results: **RT3DECHO DS showed less volume underestimation compared with 2DECHO and RT3DECHO apical rotation. Test-retest variability for RT3DECHO DS end-diastolic volume, end-systolic volume, stroke volume, and ejection fraction were 3.3%, 8.7%, 10%, and 10.3%, respectively. Normal reference ranges of indexed volumes (mean ± 2SD) for right ventricular end-diastolic volume, end-systolic volume, stroke volume, and ejection fraction were 38.6 to 92.2 mL/m², 7.8 to 50.6 mL/m², 22.5 to 42.9 mL/m², and 38.0% to 65.3%, respectively, for women and 47.0 to 100 mL/m², 23.0 to 52.6 mL/m², 14.2 to 48.4 mL/m², and 29.9% to 58.4%, respectively, for men.**

Conclusions: **RT3DECHO DS is superior to RT3DECHO apical rotation and 2DECHO for right ventricular quantification, and performs acceptably when compared with cardiac magnetic resonance imaging in healthy individuals.** (J Am Soc Echocardiogr 2007;20: 445-455.)

Accurate estimation of right ventricular (RV) size and function is essential for the management of many cardiac disorders. However, evaluation of RV function has been hampered by its complex crescentic shape, large infundibulum, and trabecular nature. Its function by invasive angiography can be characterized using area and length measurements or Simpson's rule from single or biplane projections.[1] Single plane methods provide limited sampling of the RV, depend on the orientation of the imaging planes with respect to intrinsic RV axes, and make shape assumptions. Biplane methods provide better sampling, but are invasive and often overestimate volume. Although radionuclide ventriculography is not constrained by geometric assumptions, results have been variable and scanning requires the injection of radioactive agents.[2]

Several noninvasive single and biplane 2-dimensional (2D) echocardiographic (2DECHO) methods have been proposed.[3-8] The most common method uses the area and length from an apical 4-chamber view and an RV outflow tract view.[8] The two views are assumed to have an orthogonal relationship to each other. However, the transducer is moved from one position to another based on the sonographer's knowledge of cardiac anatomy, and orthogonality is assumed but not verified and rarely satisfied. Furthermore, a prolate-ellipsoid shape assumption is made, which also may not accurately depict RV anatomy.

Three-dimensional (3D) imaging techniques such as computed tomography[9] and cardiac magnetic resonance imaging (CMR) overcome limitations posed by other methods in that image planes are precisely defined and geometric assumptions are unnecessary.[10] However, these imaging modalities are expensive and are not widespread.

A variety of options for rapid 3D echocardiographic (3DECHO) image acquisition and reconstruction of the RV exists.[11-25] Real-time 3DECHO (RT3DECHO) using second-generation matrix-array transducers retain all the advantages of echocardiography but provide 3D spatial registration. Image quality has improved over first-generation systems, thereby offering a practical approach for assessment of the RV for the first time without the use of

From St Francis Hospital, Roslyn, and Stony Brook University.

Reprint requests: Aasha S. Gopal, MD, FACC, Stony Brook University, New York, St Francis Hospital, 100 Port Washington Blvd, Roslyn, NY 11576 (E-mail: *Aasha.Gopal@chsli.org*).

0894-7317/$32.00

doi:10.1016/j.echo.2006.10.027

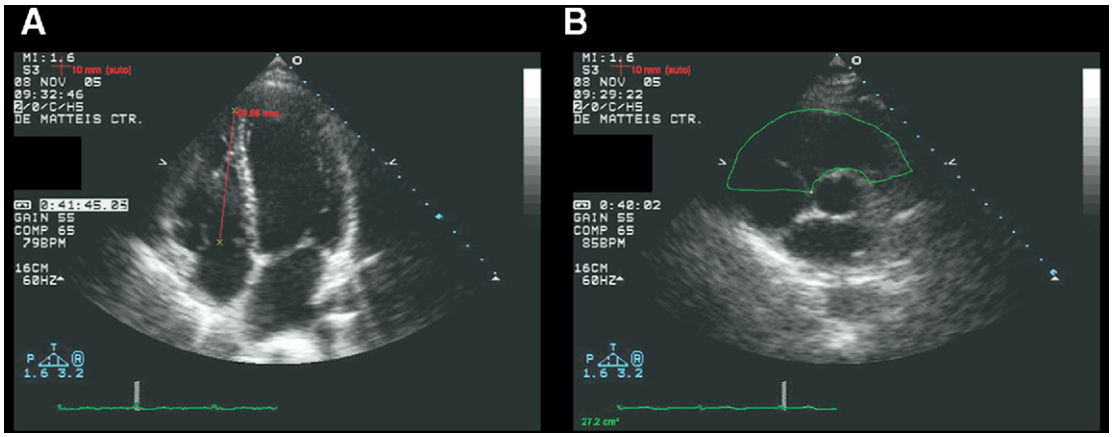

Figure 1 Two-dimensional echocardiographic long axis of right ventricle (RV) (length) (**A**) and short axis of RV infundibular area (**B**) in diastole for purposes of RV volume calculation by area-length method.

geometric assumptions. Our purpose was to establish normal values using the best RT3DECHO approach to RV quantification, and to compare it with 2DECHO methods.

Hypothesis

We hypothesized that RT3DECHO is superior to 2DECHO for assessment of RV volumes and function when compared with CMR by offering a method that does not rely on image orientation or shape assumptions.

METHODS

Recruitment of Participants

A total of 110 consecutive healthy volunteers were screened. Participants with a body mass index of 28 kg/m^2 or greater, hypertension (blood pressure ≥ 140/90 mm Hg or history of antihypertensive medication use), diabetes mellitus, symptoms or history of cardiovascular disease, anemia, thyroid or other endocrine dysfunction, neoplasia, or any other condition likely to affect cardiovascular function or body size/composition were excluded. A 2DECHO examination was performed to exclude cardiac abnormalities such as valvular dysfunction (any degree of valvular stenosis or ≥regurgitation 1+), qualitative or quantitative abnormalities of chamber sizes, systolic or diastolic function, myocardial mass, or regional wall motion. Five individuals with claustrophobia were unable to perform CMR, 18 were excluded because of 2DECHO abnormalities, 6 because of hypertension, 4 because of body mass index of 28 kg/m^2 or greater, and 6 for valvular disease. A total of 71 individuals participated in the study. No participant was excluded on the basis of image quality. CMR, 2DECHO, and RT3DECHO were performed within 24 hours to minimize the effects of biologic variability. Test-retest variability was determined for the best echocardiography method in 20 participants. Our hospital institutional review board approved the study.

Comparison of Echocardiographic Methods with CMR

2DECHO. The 2DECHO (3.2 MHz) (7500, Philips Imaging Systems, Andover, Mass) was performed with tissue harmonic imaging. A blinded operator analyzed digitized cineloops offline. The videoframe corresponding to the R wave of the electrocardiogram (ECG) was designated as end diastole. The videoframe with the smallest cavity size was designated as end systole. Papillary muscles, moderator bands, and trabeculae were included as part of the cavity volume. Endocardial boundaries were traced on the myocardial side of the black-white boundary.

Then RV measurements were taken from two planes as described by Levine et al.[8] The maximum base-to-apex length (L) in the apical 4-chamber view and the widest planimetered area (A) in the RV outflow tract view were obtained to compute volumes: V = 2/3 (A) (L) (Figure 1). Stroke volume (SV) and ejection fraction (EF) were calculated from RV end-diastolic volume (EDV) and end-systolic volume (ESV).

RT3DECHO. *RT3DECHO data acquisition.* RT3DECHO was performed using a matrix-array transducer (2−4 MHz) (X4, Philips Imaging Systems). The entire RT3DECHO data set was acquired from a single apical transducer location that was modified slightly from the traditional apical 4-chamber view such that the right-sided structures were maximized, visualized clearly, and appeared in the center of the field of view (Figure 2). A wide-angled, full-volume scan was acquired during suspended respiration at low density to maximize sector width. In this acquisition mode, 4 wedges (15 × 60 degrees) were obtained over 8 consecutive ECG-gated cardiac cycles. Because the data acquisition required ECG gating, the output was not truly real time but actually reconstructed from the subvolumes. Therefore, the entire reconstructed 3D data set was first

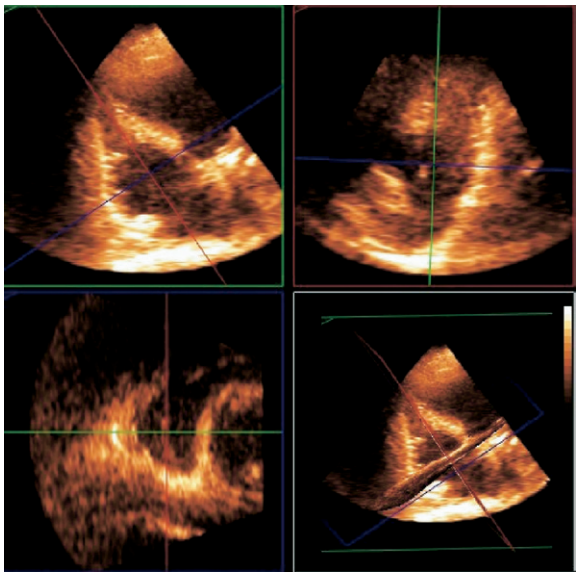

Figure 2 Real-time 3-dimensional (3D) echocardiographic data acquisition from off-axis apical window. *Top left*, *top right*, and *bottom left*, Three orthogonal multiplanar reconstructions (MPR) of right ventricle. *Bottom right*, Partial coronal view of 3D data set showing intersecting sagittal and axial planes from which MPR were derived.

inspected for whole body motion artifacts that may have occurred during data acquisition. The reconstructed data were then played as a loop and had a temporal resolution of 15 to 18 volumes/s or 55 to 65 milliseconds between successive frames. The 3D data set was also manipulated offline by a series of translational, rotational, and pivoting maneuvers to visualize the RV inflow and outflow tracts and displayed in a multiplanar reconstruction (MPR) review mode showing 3 orthogonal views (TomTec Imaging Systems GmbH, Munich, Germany) (Figure 2).

RT3DECHO volume by apical rotation. The number of image planes was then doubled successively, to obtain 8 rotationally equidistant, apical slices. The number of planes was chosen on the basis of the work of Weiss et al[26] in which underestimation was minimized by including 7 to 10 images and our own experience using this method for left ventricular volume calculations.[27] End-diastolic and end-systolic frame selection as well as boundary tracing was performed in a manner similar to 2DECHO. Traced boundaries were displayed simultaneously in 3 MPRs, which were checked for consistency by toggling back and forth and by viewing them interactively (Figure 3). Volumes were generated by an experienced blinded observer using apical rotation (AR) and surface approximation (TomTec Imaging Systems GmbH). A description of the AR surface approximation algorithm is included in the Appendix. An unblinded training set of 10 studies with known CMR values was used initially to gain experience and to establish consistent boundary tracing rules.

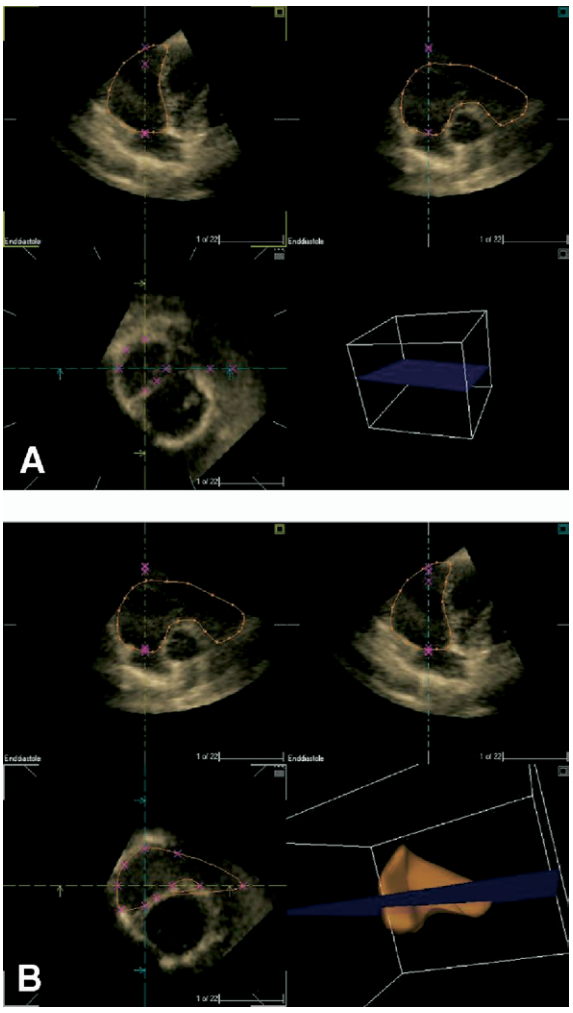

Figure 3 Real-time 3-dimensional (3D) echocardiographic apical rotation method. **A**, *Top left*, *top right*, and *bottom left*, Three orthogonal multiplanar reconstructions (MPR) of right ventricle (RV) taken at basal level showing discontinuity of RV inflow and outflow tracts. **B**, Same 3D data set shown in **A** is now advanced to show 3 orthogonal MPR (*top left*, *top right*, and *bottom left*) of RV taken at midventricular level.

RT3DECHO volume by disk summation. The MPR containing the tricuspid valve, infundibulum, and pulmonic valve in the same plane served as the basal slice of the RV. End-diastolic and end-systolic videoframe selection was performed in a manner similar to 2DECHO. Contrary to the 2DECHO area-length method in which the long-axis and infundibular short-axis views are not truly orthogonal, the MPRs obtained in the RT3DECHO method are electronically derived from the same 3D data set and, thus, have a known orthogonal relationship.

The RV was then displayed as 3 orthogonal MPRs (Figure 4). The bottom left panel of each of the figures represents an axial plane of the RV. The contour of the RV was traced manually by the operator in the axial plane.

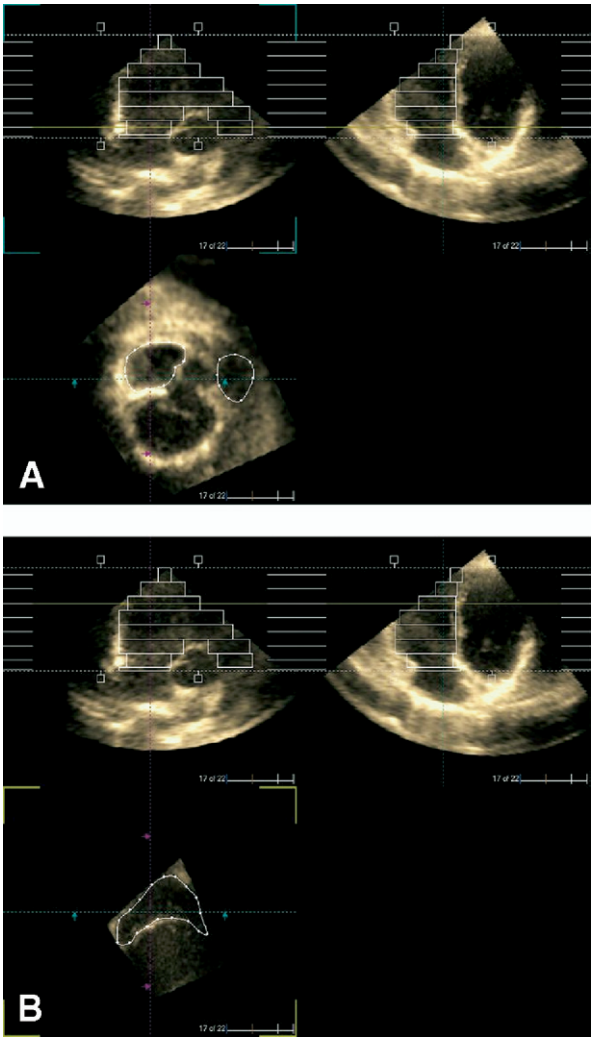

Figure 4 Real-time 3-dimensional (3D) echocardiographic disk summation method. **A**, Three orthogonal multiplanar reconstructions (MPR) of right ventricle (RV) taken at basal level showing discontinuity of RV inflow and outflow tracts. **B**, Same 3D data set shown in **A** is now advanced to show 3 orthogonal MPR of RV taken at midventricular level.

The traced contour generated bricks or disks of fixed height (10 mm) but varying lengths and widths as visualized in the top left and top right MPRs of Figure 4. The dimensions of the bricks or disks were used only as a visual aid as the traced axial contours were manipulated at each level so that the disks approximated the contours of the RV as closely as possible in the orthogonal MPRs. The volume of the RV cavity was computed by summating the known areas of the axial traces obtained 10-mm apart and the fixed height of 10 mm, ie, disk summation (DS) (TomTec Imaging Systems GmbH). The number of disks required to cover the RV from base to apex varied according heart size, but typically numbered 7 to 8 slices. Test-retest variability was computed for two separate

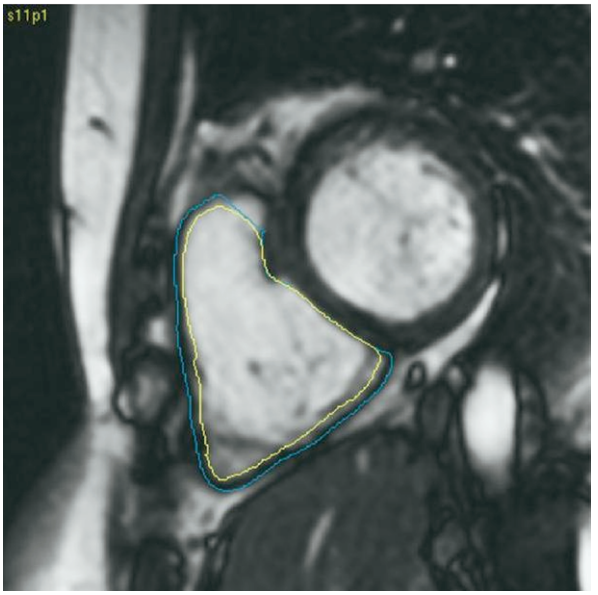

Figure 5 TruFISP cine cardiac magnetic resonance imaging of right ventricle (RV) in short axis at level of RV outflow tract.

acquisitions by comparing the tracings from two blinded observers. An unblinded training set of 10 studies with known CMR values was used initially to gain experience and to establish consistent boundary tracing rules as mentioned previously.

CMR. CMR was performed on a 1.5-T scanner (Sonata, Siemens, Erlangen, Germany). The short axis of the RV was defined and ECG-gated breath hold TruFISP obtained over the cardiac cycle with a 128-×-256 matrix, field of view of 31 to 38 cm, slices thickness of 8 mm, and temporal resolution of 40 milliseconds. RV short-axis images were obtained from the apex to above the tricuspid valve. Blinded offline analysis was performed using software (Medis Mass, Leiden, The Netherlands). Slice cavity volume was determined as the product of slice thickness and cavity area (Figure 5) and summed.

Statistical Analysis

RT3DECHO DS, RT3DECHO AR, and 2DECHO volumes were compared with CMR using Pearson's correlation, linear regression, and Bland-Altman analysis. Then sex-specific indexed (to body surface area) normal reference ranges were determined. Test-retest variability for two consecutive data acquisitions was calculated according to the formula below, where X_1 = value of observer 1, X_2 = value of observer 2, and n = 20.

$$\frac{\sqrt{\sum_1^n (X_1 - X_2)^2/n}}{\frac{1}{2}\left(\sum_1^n X_1/n + \sum_1^n X_2/n\right)}$$

Table 1 Comparison of echocardiography to cardiac magnetic resonance imaging (n = 71)

Echocardiography method	*r*	SEE, mL	Regression equation	P	Bias, mL	Agreement limits, mL	
						Lower	Upper
EDV							
2DECHO	0.3	9.1	y = 0.3x+26.9	.007	−19.5	−50.5	11.5
RT3DECHO-AR	0.8	5.7	y = 0.7x+3.4	<.0001	−16.0	−33.8	1.8
RT3DECHO-DS	0.9	4.3	y = 1.0x+1.2	<.0001	−1.2	−13.6	11.1
ESV							
2DECHO	0.1	3.0	y = 0.1x+15.1	.32	−14.7	−37.2	7.8
RT3DECHO-AR	0.8	2.5	y = 0.9x+4.6	<.0001	−8.3	−19.7	3.1
RT3DECHO-DS	0.8	8.1	y = 0.7x+23.1	<.0001	−0.02	−11.7	11.6
SV							
2DECHO	0.1	4.4	y = 0.1x+27.3	.19	−4.8	−26.3	16.7
RT3DECHO-AR	0.6	3.4	y = 0.5x+11.6	<.0001	−7.6	−22.7	7.4
RT3DECHO-DS	0.8	3.0	y = 0.9x+4.2	<.0001	−1.2	−12.5	10.1
EF							
2DECHO	0.2	4.4	y = 0.1x+70.3	.18	11.1	−11.8	34.0
RT3DECHO-AR	0.7	4.7	y = 0.7x+16.2	<.0001	−1.7	−11.9	15.3
RT3DECHO-DS	0.8	4.5	y = 0.9x+7.1	<.0001	−0.7	−13.3	11.8

AR, Apical rotation; *DS*, disk summation; *EDV*, end-diastolic volume; *EF*, ejection fraction; *ESV*, end-systolic volume; *RT3DECHO*, real-time 3-dimensional echocardiography; *SEE*, standard error of the estimate; *SV*, stroke volume; *2DECHO*, 2-dimensional echocardiography.

RESULTS

Of the 71 participants, 36 were female; mean age was 56 ± 14.3 years. Mean indexed CMR RV EDV, ESV, SV, and EF were 71.3 ± 12.9, 33.5 ± 9.9, 37.8 ± 8.7 mL/m^2, and 53.3 ± 9.0%, respectively.

We compared echocardiography measurements with CMR values (Table 1). There was a statistically significant correlation between 2DECHO RV EDV and CMR, but none between 2DECHO RV ESV, SV, EF, and CMR. RT3DECHO DS (r = 0.9 for EDV, r = 0.8 for ESV, r = 0.8 for SV, r = 0.8 for EF) and RT3DECHO AR (r = 0.8 for EDV, r = 0.8 for ESV, r = 0.6 for SV, r = 0.7 for EF) correlated significantly with corresponding CMR values and were superior to 2DECHO (r = 0.3 for EDV, r = 0.1 for ESV, r = 0.1 for SV, r = 0.2 for EF) with lower standard errors of the estimate and narrower limits of agreement. The Bland-Altman analysis revealed greater underestimation of volumes by 2DECHO compared with both RT3DECHO methods using CMR as a reference. The EF conversely was overestimated by 2DECHO when compared with CMR.

RT3DECHO DS resulted in the best agreement with CMR with the least underestimation of volumes compared with RT3DECHO AR and was then used to generate sex-specific normal values indexed to body surface area (Table 2). Mean normal values for RT3DECHO DS RV EDV, ESV, SV, and EF were 65.4 ± 13.4 mL/m^2, 29.2 ± 10.7 mL/m^2, 36.1 ± 6.8 mL/m^2, and 56.2 ± 9.1%, respectively, for women. Hence, normal reference ranges of indexed volumes (mean ± 2SD) for RV EDV, ESV, SV, and EF were 38.6 to 92.2 mL/m^2, 7.8 to 50.6 mL/m^2, 22.5 to 42.9 mL/m^2, and 38.0% to 65.3%, respectively, for women. Mean normal values for RT3DECHO DS RV EDV, ESV, SV, and EF were 74.7 ± 13.0 mL/m^2, 37.8 ± 7.4 mL/m^2, 37.0 ± 11.4 mL/m^2, and 48.9 ± 9.5%, respectively, for men. Hence, normal reference ranges of indexed volumes (mean ± 2SD) for RV EDV, ESV, SV, and EF were 47.0 to 100 mL/m^2, 23.0 to 52.6 mL/m^2, 14.2 to 48.4 mL/m^2, and 29.9% to 58.4%, respectively, for men. Test-retest variability for the RT3DECHO DS was 3.3%, 8.7%, 10%, and 10.3% for RV EDV, ESV, SV, and EF, respectively.

DISCUSSION

Estimation of RV size and function is of central importance for the management of various congenital diseases.[28] Echocardiography variables that reflect the severity of right heart failure in primary pulmonary hypertension may help identify patients appropriate for more intensive therapy or earlier transplantation.[29] Assessment of RV function is also important in determining treatment options for patients with pulmonary embolism, myocardial infarction, and heart failure.[30,31] Therefore, an accurate, easily repeated, noninvasive method would be ideal for the serial evaluation of patients.

Limitations of 2DECHO

Several efforts have been made to find echocardiography methods based on simple geometric models,[4,7,8,32-34] or on multiplane methods based on Simpson's rule.[5,6,35] Although area-length methods work in vitro and in animal models, they have wide confidence limits in human beings when compared with methods, which are not subject to geometric assumptions.[36] Moreover, the geometric models

Table 2 Normal right ventricular volumes indexed to body surface area

		CMR, mL/m²			RT3DECHO-DS, mL/m²		
Volume	**n**	**Mean**	**SD**	**Reference range, mean ± 2SD**	**Mean**	**SD**	**Reference range, mean ± 2SD**
EDV							
All	71	71.3	12.9	45.5-97.1	70.0	13.9	42.2-97.8
Female	36	67.1	12.1	42.9-90.2	65.4	13.4	38.6-92.2
Male	35	75.6	12.4	50.8-100.4	74.7	13.0	48.7-100
ESV							
All	71	33.5	9.9	13.7-55.3	33.4	10.3	12.8-54.0
Female	36	28.6	8.1	12.4-44.8	29.2	10.7	7.8-50.6
Male	35	38.4	9.1	20.2-56.6	37.8	7.4	23-52.6
SV							
All	71	37.8	8.7	20.4-46.5	36.6	9.3	18-45.9
Female	38	36.2	6.8	22.6-43.0	36.1	6.8	22.5-42.9
Male	34	37.2	9.9	17.4-47.1	37.0	11.4	14.2-48.4
EF							
All	71	53.3	8.7	35.9-62	52.6	9.9	32.8-62.5
Female	38	57.5	7.0	43.5-64.5	56.2	9.1	38-65.3
Male	34	49.0	8.8	31.4-57.8	48.9	9.5	29.9-58.4

CMR, Cardiac magnetic resonance imaging; *DS*, disk summation; *EDV*, end-diastolic volume; *EF*, ejection fraction; *ESV*, end-systolic volume; *RT3DECHO*, real-time 3-dimensional echocardiography; *SV*, stroke volume.

used to describe the shape of the RV can be changed unpredictably by disease.

Wide confidence limits also occur as a result of reliance on anatomic visual information alone for determining image plane orientation. Our earlier experience using a freehand 3DECHO system that documents image position revealed wide operator variability in the optimal positioning of short-axis and apical image planes.[37] In addition, apical views are often foreshortened during 2DECHO scanning, resulting in underestimation of the RV length that is used in area-length formulas.[38] Sheehan and coworkers[24] found that standard 2DECHO monoplane and biplane RV algorithms performed better when the images were positioned correctly using 3D electromagnetic guidance.

Previous 3DECHO Approaches

Early approaches to 3D reconstruction occurred from fixed transducer positions (apical or subcostal) and used rotational or fanlike scanning. Vogel et al[16] studied 16 pediatric patients with congenital heart disease and found similar agreement with CMR as was found in our study. However, the patients were prescreened for good image quality, a prerequisite for this approach, and the method took up to 80 minutes for estimating RV SV. Fujimoto et al[17] used a rotational approach from a fixed apical position in 15 healthy volunteers (mean age 28 years) and compared the results with CMR. Their mean RV EDV and ESV values were smaller than those obtained in our study, and the degree of systematic error was greater (5%-8%) than our values (1.7%). Papavassiliou et al[18] also used a rotating 5-MHz omniplane transthoracic transducer from a fixed subcostal or apical position in 13 pediatric patients (median age 6.3 years) with congenital heart disease and found a good correlation to CMR. However, underestimation was noted for volumes greater than 100 mL. Menzel et al[39] used this approach in 11 adult patients undergoing pulmonary thromboendarterectomy. However, a failure rate of 18% was noted in the postoperative cases because of limited echocardiographic windows. Therefore, 3DECHO reconstruction from a fixed transducer position provides mechanical 3D spatial registration of cross-sectional images, but is feasible only in those who are echogenic enough to permit complete visualization of the RV from a single echocardiographic position.

Acoustic and electromagnetic tracking devices were developed to provide 3D spatial registration while scanning in a freehand fashion, permitting the sonographer to use all available echocardiographic windows.[14,24,40] Apfel et al[14] studied 26 patients with pulmonary hypertension with an acoustic spatial locating system and found a good correlation to spin-echo CMR but with 31% to 33% volume underestimation by 3DECHO. Because data acquisition occurs over several cardiac cycles in the span of 8 to 10 minutes, respiratory, whole body, or transducer motion will lead to data misregistration. Acoustic spatial locating tracking devices consist of transmitters and receivers that cannot function if there is an interruption in the line of sight between them. Electromagnetic locators are not approved for use in patients with pacing devices and may be compromised if the transmitter and receiver are not within 50 cm of each other.

Prior Work with RT3DECHO

RT3DECHO uses matrix-array transducer technology, pioneered by von Ramm and coworkers, and

permits continuous acquisition of volumetric data, thereby allowing rapid scanning and minimizing the chance of motion artifacts. Cardiac motion can be evaluated in a dynamic mode and the heart can be viewed from any desired plane. Ota et al[41] validated RV volume measurements using a first-generation RT3DECHO system in excised canine hearts and in 14 control subjects. Although their method performed accurately in vitro, their in vivo standard of comparison was not a 3D method but a 2D monoplanar modified Simpson's method. A good correlation and interobserver variability (8.3%-9.4%) was noted between 3D RV SV and monoplanar 2D SV. Shiota et al[19] validated the same technology in sheep using electromagnetic flow probes. The correlation obtained for RVSV ($r = 0.8$) was identical to that noted in our study. The Bland-Altman analysis showed a mean RV SV difference of −2.7 mL compared with −1.2 mL noted in our study. First-generation RT3DECHO systems use a sparse-array matrix transducer, which uses 256 nonsimultaneously firing elements to acquire a narrow sector angle (60 × 60 degrees) pyramidal data set. Although the 3D data set can be captured in one heartbeat, frame rates are low and image quality is relatively poor. Because of the narrow sector angle, visualization of the RV is difficult because a large portion of it is in the near field where the sector is narrowest.

Second-generation RT3DECHO systems use full matrix-array transducers using 3000 elements. This results in improved image quality, greater contrast resolution, and higher sensitivity and penetration, as well as capabilities for harmonic imaging. The full volume of the heart can be obtained by assembling 4 wedges of 15 × 60 degrees each over 8 consecutive cardiac cycles to obtain a pyramidal sector of 90 × 90 degrees. The RT3DECHO DS algorithm appears to be superior to an AR algorithm because it is able to handle data from the RV inflow and outflow tracts, which may appear to be discontinuous when viewed in a basal short-axis cross section. Whereas the RT3DECHO AR method appears to be appropriate for the simple shape of the left ventricle, it is unable to handle data in which the contours appear to overlap (Figure 3, *A*). The short-axis DS algorithm is identical to the algorithm used for analysis of CMR and is able to handle discontinuous data and overlapping contours (Figure 4, *A*). Test-retest variability for RV EDV was excellent (3.3%). Although test-retest variability for RV ESV, SV, and EF were acceptable (8.7%, 10%, and 10.3%, respectively) and comparable with those reported for CMR,[42] these values were somewhat higher than those noted for EDV, probably reflecting variability in end-systolic videoframe selection.

Comparison with CMR

Prior RT3DECHO studies have not provided a normal reference range of values. However, our range of normal indexed values is consistent with prior CMR studies, although with some differences that may be attributable to differences in CMR technique. Rominger et al,[43] using breath-hold CMR, obtained RV volumes in 52 control subjects. Normal reference ranges of indexed volumes for RV EDV and ESV were similar to those noted in our study (48-107.5 vs 42.2-97.8 mL/m^2 and 13.1-47.2 vs 12.8-54.0 mL/m^2, respectively). In another study by Alfakih et al,[44] 60 control subjects were examined by CMR using steady-state free procession. Mean indexed RV EDV was 86.2 ± 14.1 and 75.2 ± 13.8 mL/m^2 for male and female participants, respectively. The sex-based differences noted in their study were noted in ours as well. Interstudy reproducibility of RV EDV, ESV, and EF by CMR has been reported to be 6.2%, 14.1%, and 8.3%, respectively, by Grothues et al.[42] Their values are similar to those reported by RT3DECHO in our study and similar higher test-retest variability was noted for ESV as compared with EDV.

Study Limitations

Although no patients were excluded on the basis of image quality, good images were obtained in all participants, likely because of stringent prescreening body mass index criteria for normality. RT3DECHO is subject to error if the RV is large and a large portion of the infundibulum falls outside the near field afforded by the 90- × 90-degree pyramidal sector size. Thus, although this method works well in healthy individuals, its application in markedly dilated RVs has not been established. In addition, if the RV is large, undersampling can occur by the AR method because the ventricular surface is usually convex and the volume between the true surface and the surface approximated by the AR algorithm is omitted, resulting in underestimation. Underestimation may also occur because the the RV inflow and RV outflow tracts may be very large and may appear to be discontinuous when viewed on a single image plane and, therefore, not included by the volume algorithm. This can be addressed by the short-axis DS algorithm in which portions of the RV that appear discontinuous on any given plane such as the inflow and outflow tracts can be included in the volume by summating separate discontinuous disks. In addition, the thickness of the disks can be reduced to reduce interpolation of data between traced areas. Based on the work of Weiss et al,[26] significant underestimation can be minimized by including 7 to 10 images.

Variable designation of end-diastolic and end-systolic frames by RT3DECHO and CMR is a source of error. The diastolic frame in both modalities is closely matched because the first videoframe coinciding with the R wave on the ECG is chosen. However, the end-systolic frame is chosen on the basis of smallest cavity size by RT3DECHO, whereas

the frame showing the aortic valve in the closed position is chosen as end systole by CMR. Furthermore, there are heart rate–dependent differences in temporal resolution of RT3DECHO and CMR. The RT3DECHO data set is actually reconstructed from subvolumes that are subject to motion artifacts. They are played as a loop and have a temporal resolution of 15 to 18 volumes/s or 55 to 65 milliseconds between frames whereas that of CMR is between 35 to 50 milliseconds. In addition, the choice of a single cycle, the relatively low frame rate, and difficulty in defining end systole may all have contributed to error. Because all the participants were healthy and in sinus rhythm, it is assumed that the R-R interval variations were negligible. However, limiting the analysis to a single cycle would limit accuracy in patients with widely varying R-R intervals and rhythm abnormalities.

Differences in image acquisition approaches (RT3DECHO long-axis rotational vs CMR short-axis cross-sectional approaches) introduce different partial volume effects, which may introduce error. Endocardial boundaries may be obscured by tangential RT3DECHO apical slices, whereas variable inclusion of the right atrium and RV outflow tract may occur by CMR.

Boundary tracing error remains the largest source of error. Our previous work suggests that tracing the endocardium on the white side of the black-white boundary minimizes underestimation of RT3DECHO volumes when compared with CMR. Variable visualization of the apex can be minimized by carefully manipulating the entire 3D data set so that the largest long axis is visualized and prescribing a series of short-axis images such that they are perpendicular to the long axis. Toggling between the traced endocardial boundaries as displayed in the orthogonal MPRs minimizes erroneous boundary tracing. At the moment, boundary tracing is manual and requires approximately 1 minute per boundary. Future developments in automatic image segmentation, possibly with the help of contrast agents, may improve results.

Conclusions

RT3DECHO DS is superior to RT3DECHO AR and 2DECHO for RV quantification and performs acceptably when compared with CMR in healthy individuals because of its independence from geometric assumptions and ability to process discontinous data. Normal reference ranges of indexed volumes (mean ± 2SD) for RV EDV, ESV, SV, and EF were 38.6 to 92.2 mL/m^2, 7.8 to 50.6 mL/m^2, 22.5 to 42.9 mL/m^2, and 38.0% to 65.3%, respectively, for women. Normal reference ranges of indexed volumes (mean ± 2SD) for RV EDV, ESV, SV, and EF were 47.0 to 100 mL/m^2, 23.0 to 52.6 mL/m^2, 14.2 to 48.4 mL/m^2, and 29.9% to 58.4%, respectively, for men. Test-retest variability for the RT3DECHO DS was 3.3%, 8.7%, 10%, and 10.3% for RV EDV, ESV, SV, and EF, respectively.

Although excellent agreement and interobserver variability has been found for RV volumes and EF between RT3DECHO DS and CMR in healthy individuals, further work is necessary to demonstrate use in the setting of a clinical laboratory in which a variety of RV shapes, sizes, and pathologies are encountered.

REFERENCES

1. Ferlinz J. Measurements of right ventricular volume in man from single plane cineangiograms: a comparison to the biplane approach. Am Heart J 1977;94:87-90.
2. Kaul S, Boucher CA, Okada RD, Newell JB, Strauss HW, Pohost GM. Sources of variability in the radionuclide angiographic assessment of ejection fraction: a comparison of first-pass and gated equilibrium techniques. Am J Cardiol 1984;53:823-8.
3. Bommer W, Weinert L, Neumann A, Neef J, Mason DT, DeMaria A. Determination of right atrial and right ventricular size by two-dimensional echocardiography. Circulation 1979; 60:91-100.
4. Saito A, Ueda K, Nakano H. Right ventricular volume determination by two-dimensional echocardiography. J Cardiogr 1981;11:1159-68.
5. Ninomiya K, Duncan WJ, Cook DH, Olley PM, Rowe RD. Right ventricular ejection fraction and volumes after Mustard repair: correlation of two-dimensional echocardiograms and cineangiograms. Am J Cardiol 1981;48:317-24.
6. Watanabe T, Katsume H, Matsukubo H, Furukawa K, Ijichi H. Estimation of right ventricular volume with two-dimensional echocardiography. Am J Cardiol 1982;49:1946-53.
7. Aebischer NM, Fereno C. Determination of right ventricular volume by two-dimensional echocardiography with a crescentic model. J Am Soc Echocardiogr 1989;2:110-8.
8. Levine RA, Gibson TC, Aretz T, Gillam LD, Guyer DE, King ME, et al. Echocardiographic measurement of right ventricular volume. Circulation 1984;69:497-505.
9. Reiter SJ, Rumberger JA, Feiring AJ, Stanford W, Marcus ML. Precision of measurements of right and left ventricular volume by cine computed tomography. Circulation 1986;74: 890-900.
10. Sechtem U, Pflugfelder PW, Gould PG, Cassidy MM, Higgins CB. Measurement of right and left ventricular volumes in healthy individuals with cine MR imaging. Radiology 1987; 163:697-702.
11. Linker DT, Moritz WE, Pearlman AS. A new three-dimensional echocardiographic method of right ventricular volume measurement: in vitro validation. J Am Coll Cardiol 1986;8:101-6.
12. Buckey JC, Beattie JM, Nixon JV, Gafffney FA, Blomqvist CG. Right and left ventricular volumes in vitro by a new nongeometric method. Am J Cardiol 1987;1:227-33.
13. Jiang L, Handschumacher M, Hibberd MG, Siu SC, King ME, Weyman AE, et al. Three-dimensional echocardiographic reconstruction of right ventricular volume: in vitro comparison with two-dimensional methods. J Am Soc Echocardiogr 1994;7:150-8.
14. Apfel HD, Shen Z, Boxt LM, Barst RJ, Gopal AS, Allan LD, et al. Three-dimensional echocardiographic assessment of right ventricular volume and function in patients with pulmonary hypertension. Cardiol Young 1997;7:317-24.
15. Pini R, Giannazzo G, Di Bari M, Innocenti F, Rega L, Casolo G, et al. Transthoracic three-dimensional echocardiographic

reconstruction of left and right ventricles: in vitro validation and comparison with magnetic resonance imaging. Am Heart J 1997;133:221-9.
16. Vogel M, Gutberlet M, Dittrich S, Hosten N, Lange PE. Comparison of transthoracic three-dimensional echocardiography with magnetic resonance imaging in the assessment of right ventricular volume and mass. Heart 1997;78:127-30.
17. Fujimoto S, Mizuno R, Nakagawa Y, Dohi K, Nakano H. Estimation of right ventricular volume and ejection fraction by transthoracic three-dimensional echocardiography: a validation study using magnetic resonance imaging. Int J Card Imaging 1998;14:385-90.
18. Papavassiliou DP, Parks WJ, Hopkins KL, Fyfe DA. Three-dimensional echocardiographic measurement of right ventricular volume in children with congenital heart disease validated by magnetic resonance imaging. J Am Soc Echocardiogr 1998;11:770-7.
19. Shiota T, Jones M, Chikada M, Fleishman CE, Castellucci JB, Cotter B, et al. Real-time three-dimensional echocardiography for determining right ventricular stroke volume in an animal model of chronic right ventricular volume overload. Circulation 1998;97:1897-900.
20. Heusch A, Rubo J, Krogmann ON, Bourgeois M. Volumetric analysis of the right ventricle in children with congenital heart defects: comparison of biplane angiography and transthoracic 3-dimensional echocardiography. Cardiol Young 1999;9:577-84.
21. Hubka M, Mantei K, Bolson E, Coady K, Sheehan F. Measurement of right ventricular mass and volume by three-dimensional echocardiography by freehand scanning. Comput Cardiol 2000;27:703-6.
22. Schindera ST, Mehwald PS, Sahn DJ, Kecicioglu D. Accuracy of real-time three-dimensional echocardiography for quantifying right ventricular volume: static and pulsatile flow studies in an anatomic in vitro model. J Ultrasound Med 2002;21:1069-75.
23. Angelini ED, Homma S, Pearson G, Holmes JW, Laine AF. Segmentation of real-time three-dimensional ultrasound for quantification of ventricular function: a clinical study on right and left ventricles. Ultrasound Med Biol 2005;31:1143-58.
24. Dorosz JL, Bolson EL, Waiss MS, Sheehan FH. Three-dimensional visual guidance improves the accuracy of calculating right ventricular volume with two-dimensional echocardiography. J Am Soc Echocardiogr 2003;16:675-81.
25. Wang J, Wang X, Xie M, Yang Y, Wang L. Evaluation of right ventricular volume and systolic function by real-time three-dimensional echocardiography. J Huazhong Univ Sci Technol Med Sci 2005;25:94-9.
26. Weiss JL, Eaton LW, Kallman CH, Maughan WL. Accuracy of volume determination by two-dimensional echocardiography defining requirements under controlled conditions in the ejecting canine left ventricle. Circulation 1982;67:889-95.
27. Gopal AS, Krishnaswamy RR, Toole RS, Petillo F, Schapiro W, Reichek N. Analysis requirements for practical use of live 3D echocardiography: how much is really necessary? J Am Soc Echocardiogr 2004;17:498.
28. Tulevski II, Dodge-Khatami A, Groenink M, van der Wall EE, Romkes H, Mulder BJ. Right ventricular function in congenital cardiac disease: noninvasive quantitative parameters for clinical follow-up. Cardiol Young 2003;13:397-403.
29. Eysmann SB, Palevsky HI, Reichek N, Hackney K, Douglas PS. Two-dimensional and Doppler-echocardiographic and cardiac catheterization correlates of survival in primary pulmonary hypertension. Circulation 1989;80:353-60.
30. Quiroz R, Kucher N, Schoepf UJ, Kipfmueller F, Solomon SD, Costello P, et al. Right ventricular enlargement on chest computed tomography: prognostic role in acute pulmonary embolism. Circulation 2004;109:2401-4.
31. Zornoff LAM, Skali H, Pfeffer MA, St John Sutton M, Rouleau JL, Lamas GA, et al. Right ventricular dysfunction and risk of heart failure and mortality after myocardial infarction. J Am Coll Cardiol 2002;39:1450-5.
32. Czegledy FP, Katz J. A new geometric description of the right ventricle. J Biomed Eng 1993;15:387-91.
33. Gibson TC, Miller SW, Aretz T, Hardin NJ, Weyman AE. Method for estimating right ventricular volume by planes applicable to cross-sectional echocardiography: correlation with angiographic formulas. Am J Cardiol 1985;55:1584-8.
34. Tomita M, Masuda H, Sumi T, Shiraki H, Gotoh K, Yagi Y, et al. Estimation of right ventricular volume by modified echocardiographic subtraction method. Am Heart J 1992;123:1011-22.
35. Trowitzsch E, Colan SD, Sanders SP. Two-dimensional echocardiographic estimation of right ventricular area change and ejection fraction in infants with systemic right ventricle (transposition) of the great arteries or hypoplastic left heart syndrome. Am J Cardiol 1985;55:1153-7.
36. Denslow S, Wiles HB. Right ventricular volumes revisited: a simple model and simple formula for echocardiographic determination. J Am Soc Echocardiogr 1998;11:864-73.
37. King DL, Harrison MR, King DL Jr, Gopal AS, Kwan OL, DeMaria AN. Ultrasound beam orientation during standard two-dimensional imaging: assessment by three-dimensional echocardiography. J Am Soc Echocardiogr 1992;5:569-76.
38. Erbel R, Schweizer P, Lambertz H, Henn G, Meyer J, Krebs W, et al. Echoventriculography: a simultaneous analysis of two-dimensional echocardiography and cineventriculography. Circulation 1983;67:205-15.
39. Menzel T, Kramm T, Bruckner A, Mohr-Kahaly S, Mayer E, Meyer J. Quantitative assessment of right ventricular volumes in severe chronic thromboembolic pulmonary hypertension using transthoracic three-dimensional echocardiography: changes due to pulmonary thromboendarterectomy. Eur J Echocardiogr 2002;3:67-72.
40. Leotta DF, Munt B, Bolson EL, Kraft C, Martin RW, Otto CM, et al. Quantitative three-dimensional echocardiography by rapid imaging from multiple transthoracic windows: in vitro validation and initial in vivo studies. J Am Soc Echocardiogr 1997;10:830-9.
41. Ota T, Fleishman CE, Strub M, Stetten G, Ohazama CJ, von Ramm OT, et al. Real-time, three-dimensional echocardiography: feasibility of dynamic right ventricular volume measurement with saline contrast. Am Heart J 1999;137:958-66.
42. Grothues F, Moon JC, Bellenger NG, Smith GS, Klein HU, Pennell DJ. Interstudy reproducibility of right ventricular volumes, function, and mass with cardiovascular magnetic resonance imaging. Am Heart J 2004;147:218-23.
43. Rominger MB, Bachmann GF, Pabst W, Rau WS. Right ventricular volumes and ejection fraction with fast cine MR imaging in breath-hold technique: applicability, normal values from 52 volunteers, and evaluation of 325 adult cardiac patients. J Magn Reson Imaging 1999;10:908-18.
44. Alfakih K, Plein S, Thiele H, Jones T, Ridgway JP, Sivananthan MU. Normal human left and right ventricular dimensions for MRI as assessed by turbo gradient echo and steady-state free procession imaging sequence. J Magn Reson Imaging 2002;17:323-9.

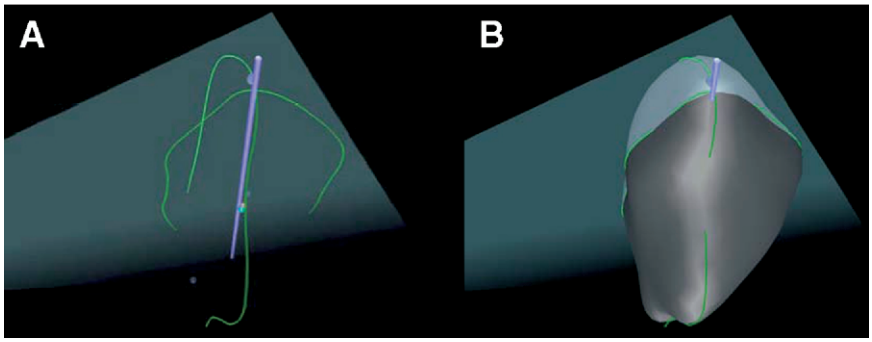

Figure 6 Real-time 3-dimensional (3D) echocardiographic apical rotation surface approximation generation of Beutel surface. **A**, For each single phase, it is accomplished by reconstructing endocardial contours of all different acquisition planes in 3D space. **B**, Smooth spherical spline model based on radial basis functions is applied to approximate parameterized contour points with minimum root mean square error. Error is measured as euclidean distance between contour point and corresponding surface point.

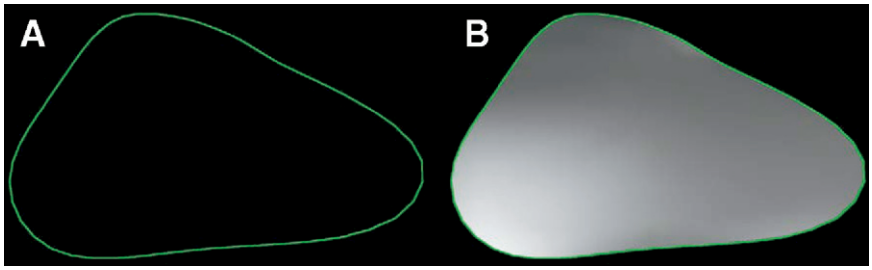

Figure 7 Real-time 3-dimensional echocardiographic apical rotation surface approximation generation of cap surface. **A**, Closed boundary curve of previously generated Beutel surface is extracted. **B**, Planar spline model based on radial basis functions is applied to interpolate all curve points with curvature minimizing surface patch.

45. Messner AM, Taylor CG. Algorithm 550 solid polyhedron measures. The Transactions on Mathmatical Software 1980; 6:121-30.

APPENDIX

VOLUME CALCULATION BY APICAL ROTATION AND SURFACE APPROXIMATION

Volume calculation by apical rotation and surface approximation occurs in 3 steps as described below.

Generation of the Beutel surface: the following description of surface reconstruction refers to each single phase.

1. Endocardial contours of all the different acquisition planes are reconstructed in 3-dimensional space (Figure 6, *A*).
2. A 2-dimensional vector parameter (u,v) is assigned to all contour points according to their relative spatial relationship (similar to longitude and latitude).
3. A smooth spherical spline model based on radial basis functions is applied to approximate the parameterized contour points with minimum root mean square error. This yields a surface model of the left ventricular cavity, called the Beutel surface. Error is measured as the euclidean distance between contour point and corresponding surface point (Figure 6, *B*).

Note that the surface models the endocardium only, ie, the surface has an opening that corresponds to the mitral valve orifice.

GENERATION OF THE CAP SURFACE

To close the Beutel surface, no model of the mitral valve is used, as the valve opens and closes during the cardiac cycle. While the valve is closed, the true mitral valve geometry is used for closure. However,

for the remaining time some closing cap surface must be defined to compute the enclosed volume. Thus, discontinuities in the volume over time curves would arise when switching between true mitral valve geometry and cap surface. Therefore, a curvature minimizing cap surface is applied for all phases. Note that this induces slightly different end-diastolic and end-systolic volumes compared with static volume measurements where the closed valve is included in the contour tracing. The following steps are performed to define the cap surface for each Beutel.

1. The closed boundary curve of the previously generated Beutel surface is extracted (Figure 7, *A*).
2. A planar spline model based on radial basis functions is applied to interpolate all curve points with a curvature minimizing the surface patch (cap surface of Beutel, Figure 7, *B*).

POLYHEDRON MEASURES

Volume computation is performed based on the work of Messner and Taylor.[45]

Using the gauss divergence theorem

$$\iiint div\bar{F}dV = \iint \bar{F}\cdot\bar{n}\,dS$$

volume integrals can be transformed to equivalent surface integrals by defining an appropriate vector field.

Example mass (or volume for $\rho = 1$):

The mass of a solid body ρ in Cartesian coordinates with constant density can be computed as:

$$M = \iiint \rho\, dV$$

Let a vector field be defined as

$$\bar{F} = \frac{\rho}{3}(x\bar{e}_x + y\bar{e}_y + z\bar{e}_z)$$

with unit vectors in direction of the coordinate axes e_i. The divergence is then:

$$div\,\bar{F} = \frac{\rho}{3}\left(\frac{\partial x}{\partial x} + \frac{\partial y}{\partial y} + \frac{\partial z}{\partial z}\right) = \rho$$

Thus the mass can be rewritten as

$$M = \iint \bar{F}\cdot\bar{n}dS = \iint \frac{\rho}{3}(x\bar{e}_x + y\bar{e}_y + z\bar{e}_z)\cdot\bar{n}\,dS$$

$$= \iint \frac{\rho}{3}(xn_x + yn_y + zn_z)dS$$

We obtain the enclosed volume for $\rho = 1$.

Correction

The following article was published with the incorrect list of authors in the online version of the January 2007 issue of Journal of American Society of Echocardiography: *Burgess MI, Fang ZY, Marwick TH. Role of diastolic dyssynchrony in the delayed relaxation pattern of left ventricle filling. J Am Soc Echocardiogr 2007;20:63-69.* This error has been corrected. We apologize for any inconvenience or confusion this error has caused.